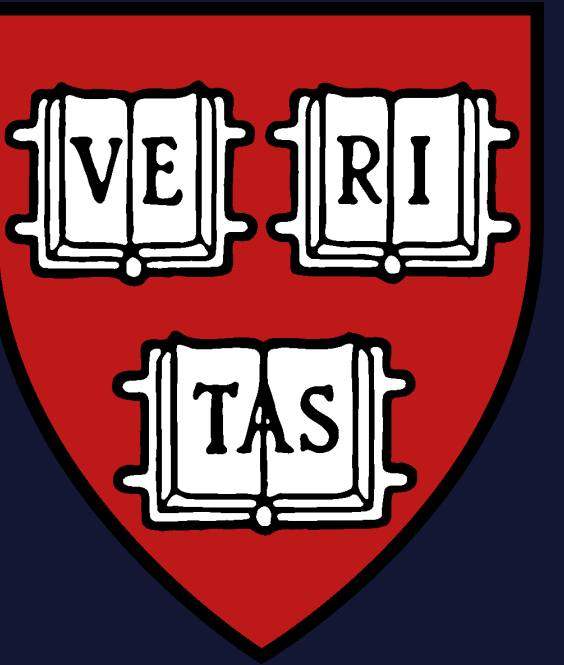


# Doppler Tomograms of X-ray Binary Systems V801 Ara and Cyg X-3 from Optical and Near-Infrared Spectroscopy



Kaley Brauer<sup>1,2</sup>, Saeqa Vrtilek<sup>2</sup>, Charith Peris<sup>2</sup>, Karri Koljonen<sup>3</sup>, Michael McCollough<sup>2</sup>

<sup>1</sup>Brown University, Providence, RI, USA; <sup>2</sup>Harvard-Smithsonian, CfA, Cambridge, MA, USA; <sup>3</sup>Finnish Center for Astronomy, Turku, Finland

## Introduction

We have observations of two X-ray binary systems: optical IMACS spectra of V801 Ara and near-infrared GNIRS spectra of Cyg X-3. Both sets of spectra show a multitude of emission features that contain information about the structures of the systems, and **we have selected several lines from each system to analyze with Doppler tomography**.

V801 Ara is a persistent X-ray binary system comprising a neutron star and a late-type, low-mass companion star<sup>1</sup>. Casares et al. (2006) conducted Doppler tomography of V801 Ara on the emission features He II  $\lambda 4686$  and the Bowen fluorescence N III  $\lambda 4640$ <sup>2</sup>. They identified the companion star as the source of N III  $\lambda 4640$  and were able to provide estimates for the radial velocities and the mass ratio of the system. In addition to revisiting these emission features, we expand on the work of Casares et al. (2006) by producing the first tomograms of V801 Ara in H $\alpha$  and H $\beta$ .

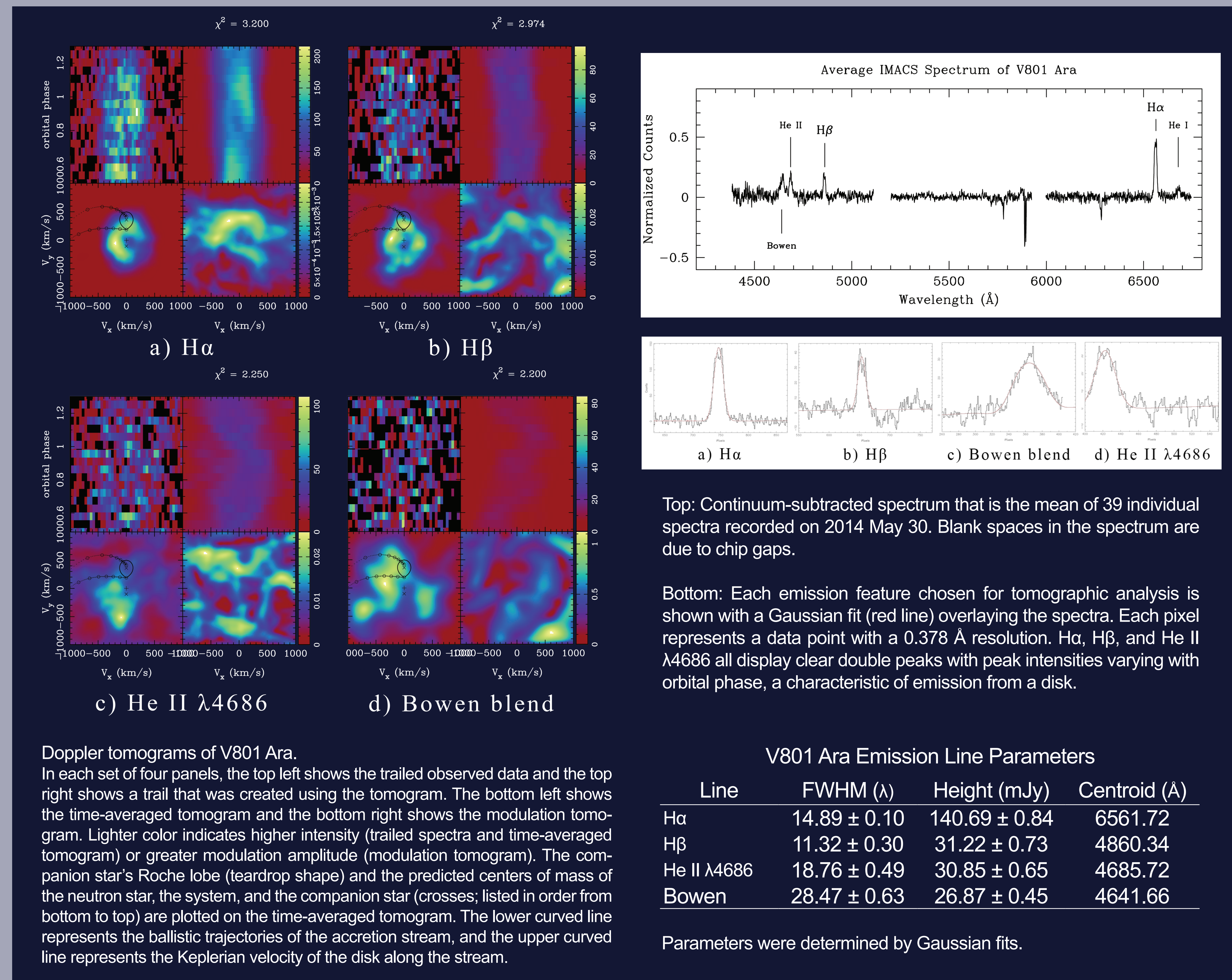
Cygnus X-3 is a binary system comprising a WN5-7 type Wolf-Rayet star<sup>3</sup> and either a black hole or a neutron star. Previous tomography of Cyg X-3 was carried out by Hanson, Still, & Fender (2000); this work resulted in an estimate of the mass function of the system<sup>4</sup>. We expand on this work by probing multiple He II and N lines.

## Methods

**Doppler tomography<sup>5</sup> can be used to probe the structure and variability of line-emitting or line-absorbing regions in binary systems.** Tomograms are two-dimensional maps in velocity space requiring line profiles obtained at frequent intervals around a full orbital period. The Doppler broadening of the line profile contains information about the velocity distribution, and the rotation of the system supplies a continuous series of projections from which a tomogram can be formed.

We prepared both sets of spectra for tomographic analysis by fitting a curve to the continuum, subtracting the curve from each spectrum, and isolating each emission feature. **To create the tomograms, we used an iterative reduced  $\chi^2$  process** that modified a simple starting image (a uniform grid or a Gaussian) to fit the data by gradually decreasing the reduced  $\chi^2$  in comparison to the data. Because many possible fits exist for a given  $\chi^2$ , the Maximum Entropy Method<sup>6</sup> was used to select the most realistic fit. The Maximum Entropy Method, based on the idea that higher entropy corresponds to a smoother and more physically probable image, involves selecting the fit with the highest entropy after each iteration.

## V801 Ara



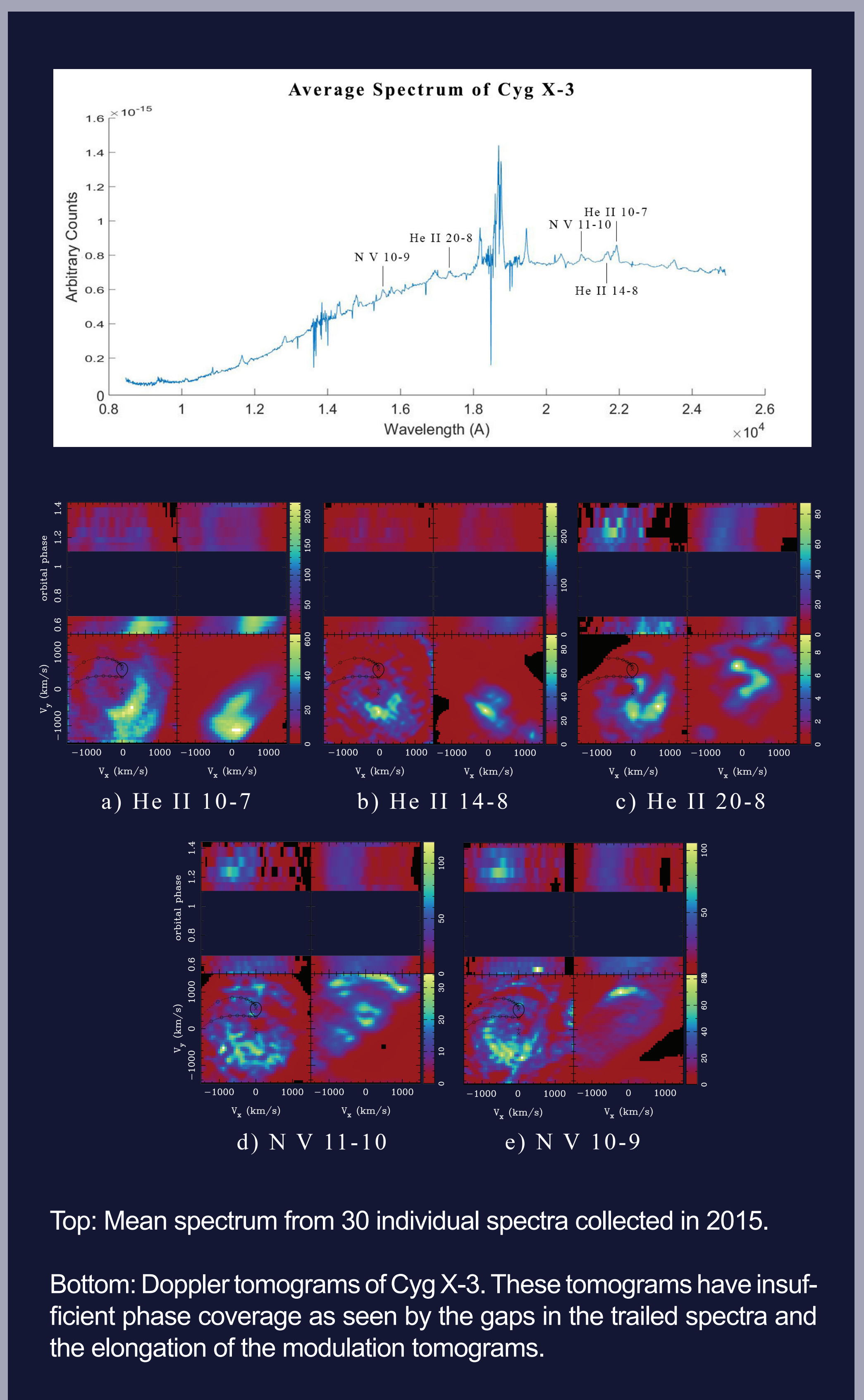
Standard Doppler tomography produces time-averaged tomograms. Modulation Doppler tomography<sup>7</sup>, an extension of standard Doppler tomography, allows for investigation of time-dependent variations in the line profiles. Modulation tomography takes into account how the flux from a given point varies as a function of time and produces a tomogram showing emission sources that harmonically vary as a function of the period. We employed both modulation tomography and standard tomography when producing our tomograms.

We used ephemerides from Casares et al. (2006) and Singh et al. (2002) in our analysis<sup>2,8</sup>, and K1, K2, and  $\gamma$  values from Casares et al. (2006) and Hanson, Still, & Fender (2000) when plotting predicted center of mass values on the tomograms<sup>2,4</sup>.

## Discussion

**The V801 Ara tomograms constructed using H $\alpha$  and H $\beta$  allow us to identify the accretion disk.** The center of the disk does not appear to coincide with the center-of-mass of the neutron star, however, but rather coincides with the center-of-mass of the system. **This offset has been associated with eccentric accretion disks<sup>9</sup>.** We cannot be certain that V801 Ara has an eccentric disk until the K1 and K2 values are better constrained, however. Additionally, we did not detect a hot spot at the point where the accretion stream is expected to hit the disk (between the lines representing the accretion stream and the velocity along the disk), **implying that V801 Ara is in a low accretion state.**

## Cyg X-3



Our V801 Ara tomograms of N III  $\lambda 4640$  and He II  $\lambda 4686$  were less reliable due to our inability to fit the continuum on both sides. We also find that the trailed spectra computed from inverting the tomogram do not match the real trailed spectrum as well as the H $\alpha$  and H $\beta$  tomograms. The N III  $\lambda 4640$  tomogram shows some emission at the location of the companion star as found by Casares et al. (2006), but it also shows emission elsewhere so that we cannot confirm detection of the companion.

**Due to a large gap in phase coverage, we were unable to produce significant tomograms of Cyg X-3.** The elongation of the features in the modulation tomograms is an indication of insufficient phase coverage. To finish the analysis, we applied for further time from Gemini North to obtain more observations.

[1] Fujimoto, M. Y., & Taam, R. E. 1986, ApJ, 305, 246, [2] Casares, J., Cornelisse, R., Steeghs, D., et al. 2006, MNRAS, 373, 1235, [3] van Kerkwijk, M. H., Charles, P. A., Geballe, T. R., et al. 1992, Nature, 355, 703, [4] Hanson, M. M., Still, M. D., & Fender, R. P. 2000, ApJ, 541, 308, [5] Marsh, T. R. 2005, Ap&SS, 296, 403, [6] Narayan, R., & Nityananda, R. 1986, ARA&A, 24, 127, [7] Steeghs, D. 2003, MNRAS, 344, 448, [8] Singh, N.S., Naik, S., Paul, B., et al. 2002, A&A, 392, 161, [9] Neilsen, J., Steeghs, D., & Vrtilek, S. D. 2008, MNRAS, 384, 849